

Coherent Electrical Activity Between Vibrissa Sensory Areas of Cerebellum and Neocortex Is Enhanced During Free Whisking

SEAN M. O'CONNOR,¹ RUNE W. BERG,¹ AND DAVID KLEINFELD^{1,2}

¹Department of Physics and ²Neurosciences Graduate Program, University of California at San Diego, La Jolla, California 92093

Received 19 March 2001; accepted in final form 6 December 2001

O'Connor, Sean M., Rune W. Berg, and David Kleinfeld. Coherent electrical activity between vibrissa sensory areas of cerebellum and neocortex is enhanced during free whisking. *J Neurophysiol* 87: 2137–2148, 2002; 10.1152/jn.00229.2001. We tested if coherent signaling between the sensory vibrissa areas of cerebellum and neocortex in rats was enhanced as they whisked in air. Whisking was accompanied by 5- to 15-Hz oscillations in the mystacial electromyogram, a measure of vibrissa position, and by 5- to 20-Hz oscillations in the differentially recorded local field potential (VLFP) within the vibrissa area of cerebellum and within the VLFP of primary sensory cortex. We observed that only 10% of the activity in either cerebellum or sensory neocortex was significantly phase-locked to rhythmic motion of the vibrissae; the extent of this modulation is in agreement with the results from previous single-unit measurements in sensory neocortex. In addition, we found that 40% of the activity in the vibrissa areas of cerebellum and neocortex was significantly coherent during periods of whisking. The relatively high level of coherence between these two brain areas, in comparison with their relatively low coherence with whisking per se, implies that the vibrissa areas of cerebellum and neocortex communicate in a manner that is incommensurate with whisking. To the extent that the vibrissa areas of cerebellum and neocortex communicate over the same frequency band as that used by whisking, these areas must multiplex electrical activity that is internal to the brain with activity that is that phase-locked to vibrissa sensory input.

INTRODUCTION

The operation of a sensorimotor system may involve signals that are directly locked to sensory input or motor output as well as signals that are used solely for internal communication between different brain areas. In principal, these two types of signals may be coded so that they share the same frequency bands yet remain incoherent with each other (Izhikevich 1999; Viterbi 1995). Precedence for internal signaling that is incommensurate with the stimulus occurs in the visuomotor systems of cat (Eckhorn et al. 1988; Gray et al. 1989; Roelfsema et al. 1997), monkey (Friedman-Hill et al. 2000; Fries et al. 2001; Kreiter and Singer 1996), and turtle (Prechtl 1994; Prechtl et al. 1997). However, there is apparently no precedence for internal signaling that shares the same frequency band as the stimulus. To address this possibility, we focus on the nature of electrical signaling within different brain areas of the vibrissa sensorimotor system of rat (for review, see Kleinfeld et al. 1999).

Address for reprint requests: D. Kleinfeld, Dept. of Physics 0319, University of California, 9500 Gilman Dr., La Jolla, CA 92093 (E-mail: dk@physics.ucsd.edu).

The vibrissae are tactile sensors whose angular position is controlled by the follicles in the mystacial pad. Each follicle is innervated by neurons from the trigeminal sensory ganglion, while motion of the follicles is under control of intrinsic and extrinsic mystacial muscles, both of which receive input from the facial motor nucleus (Dorfl 1982, 1985) (Fig. 1). These sensory and motor structures are linked via the trigeminal nuclei and form a closed loop at the level of the hindbrain (hindbrain loop, Fig. 1). The hindbrain loop is nested within a loop that encompasses the pontine- and olivocerebellar nuclei and integrates input from the trigeminal nuclei as well as higher brain areas. The cerebellar nuclei project to the superior colliculus and subsequently to the facial motor nucleus to form a closed loop at the level of the midbrain (midbrain loop, Fig. 1). The highest level feedback loop in the vibrissa sensorimotor system involves structures at the level of the forebrain. Sensory projections from the trigeminal nuclei travel up through dorsal thalamus and primary sensory (S1) and motor areas of cortex and then down to both the colliculus and directly to reticular nuclei (Miyashita et al. 1994) to close the loop (forebrain loop, Fig. 1).

Here we ask: what is the extent of coherent electrical activity between individual vibrissa sensory areas and vibrissa motion during whisking? How does this stimulus-locked coherence compare with the internal coherence between the different brain areas? As a means to address these questions, we recorded the mystacial electromyogram (EMG; Fig. 1), which reports the output of vibrissa motoneurons in the facial nucleus (Carvell et al. 1991; Klein and Rhoades 1985), along with the spatially localized field potential from the vibrissa sensitive region of the cerebellum (cerebellar VLFP; Fig. 1) and the spatially localized field potential from the vibrissa sensitive region of S1 cortex (cortical VLFP; Fig. 1). A crucial aspect of our experiments was the use of animals that were trained to whisk in air for extended periods (Fee et al. 1997). This provided a high fidelity and unambiguous behavioral reference signal, particularly because the phase of whisking may drift over successive cycles.

METHODS

Animals

Seven female Long Evans rats (Charles River, ME), 270–300 g initial weight, served as subjects. Four animals provided data for our

The costs of publication of this article were defrayed in part by the payment of page charges. The article must therefore be hereby marked “advertisement” in accordance with 18 U.S.C. Section 1734 solely to indicate this fact.

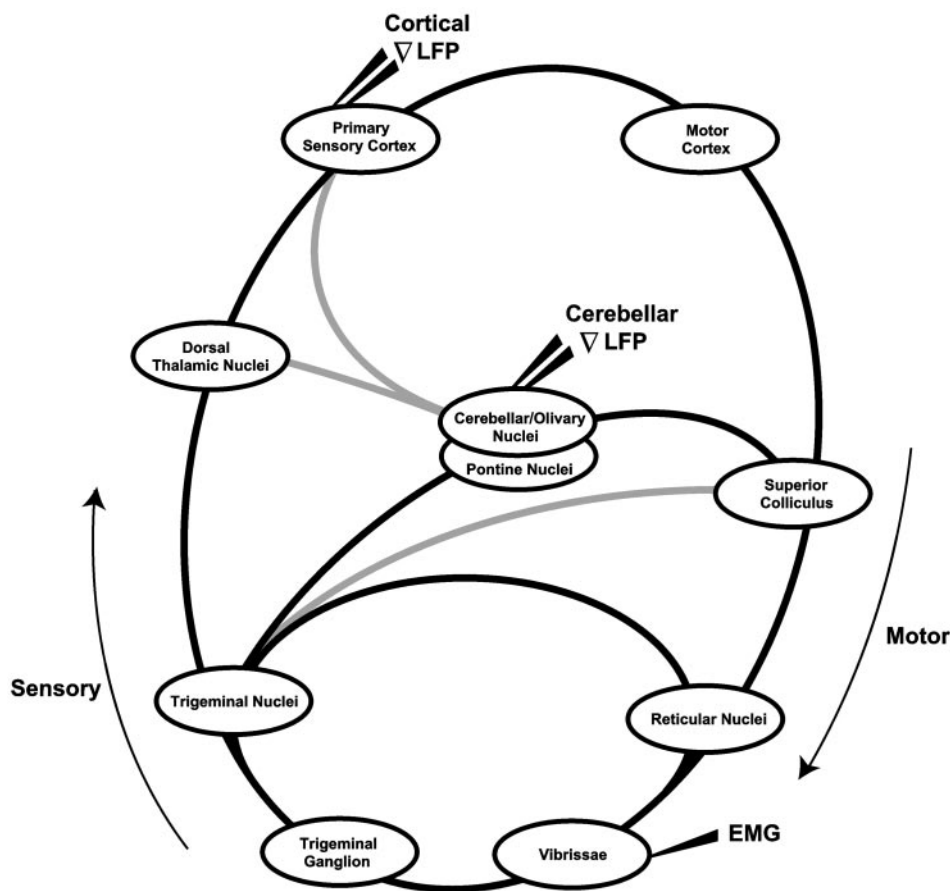


FIG. 1. Cartoon of the vibrissa sensorimotor system including structures in the hindbrain, cerebellar, and cortical loops that are relevant to this study. We review the loops that are directly relevant to the present work (black lines); details and a complete set of references are summarized in Kleinfeld et al. (1999). Hindbrain/medulla loop: the vibrissae are innervated by 2 kinds of sensory afferents that originate from the infraorbital nerve and form the projection from vibrissae to the trigeminal ganglion. Sensory input from the trigeminal ganglion enters the hindbrain at the trigeminal nuclei, consisting of the principal sensory nucleus and three spinal trigeminal nuclei. One projection from the trigeminal nuclei is to the lateral facial subnuclei in the reticular formation. Midbrain/cerebellar loop: the trigeminal nuclei provide vibrissa sensory input to the cerebellum via 2 paths, the inferior olive climbing fibers and the pontine mossy fibers. A 3rd input pathway is provided via primary sensory (S1) cortex (gray line). The deep cerebellar nuclei send a projection to the colliculus to complete a vibrissa loop. Note that the superior colliculus also sends a projection back to the cerebellar cortex through both the inferior olive and the pons to form a closed cerebellum-colliculus feedback path. Forebrain loop: all trigeminal nuclei send projections to the ventral posteromedial and posterior nuclei in dorsal thalamus. These thalamic regions project to S1 cortex, secondary areas of sensory neocortex that send feedback projections to dorsal thalamus and the trigeminal nuclei. Vibrissa S1 cortex forms reciprocal projections with other vibrissa sensory areas and with primary motor (M1) cortex. Motor as well as sensory neocortex send descending projections to the superior colliculus. A direct connection from vibrissa motor neocortex to multiple nuclei in the reticular formation adjacent to the facial nucleus is suggestive of a central pattern generator (Hattox et al. 2001).

mapping studies, and three animals provided data for our extracellular measurements on behaving animals. The care and experimental manipulation of our animals were in strict accord with guidelines from the National Institutes of Health (1985) and have been reviewed and approved by the Institutional Animal Care Committee at UCSD.

Mapping the cerebellar response

The rat was placed under halothane anesthesia [1–2% (vol/vol) in O_2 at a flow rate of 500–1,000 SCCM], and a craniotomy was performed to expose an $\sim 4 \times 6$ -mm region of cerebellar cortex that incorporated crus 1 and 2. Maps of the electrical response, obtained with etched Tungsten microelectrodes ($|Z(f = 1 \text{ kHz})| \approx 1 \text{ M}\Omega$; WE300325A, Micro Probe), were obtained in response to repeated manual taps to one or two vibrissae. Responses were characterized as “strong,” “weak,” or absent based on the relative amplitude of the audible spike signal.

Behavioral training and chronic recording

Rats were habituated to human touch and the behavioral apparatus. After several weeks, both extracellular cortical and EMG electrodes were surgically implanted with the rat under halothane anesthesia [2–3% (vol/vol) in O_2]. In brief, the skull above the vibrissa areas of cerebellar and parietal cortex in both hemispheres was exposed and cleared of soft tissue. Thin cement (Superbonder 49550; Loctite) was spread across the remaining skull surface, and small bolts (No. 00-90) were implanted into the skull to act as anchors for the electrodes. Microwire electrodes were prepared from Teflon-coated tungsten wire (0.002-in; No. 7955, A-M Systems) that was cut and polished on the diagonal. Individual microwires were implanted stereotaxically in the cerebellum (Fig. 2A), as delineated from our mapping studies, in parietal cortex to record from the part of the vibrissa area of S1 that is sensitive to the central, rostral vibrissae (e.g., vibrissae C_1 – C_3) (Chapin and Lin 1984). Two or three electrodes were implanted in the

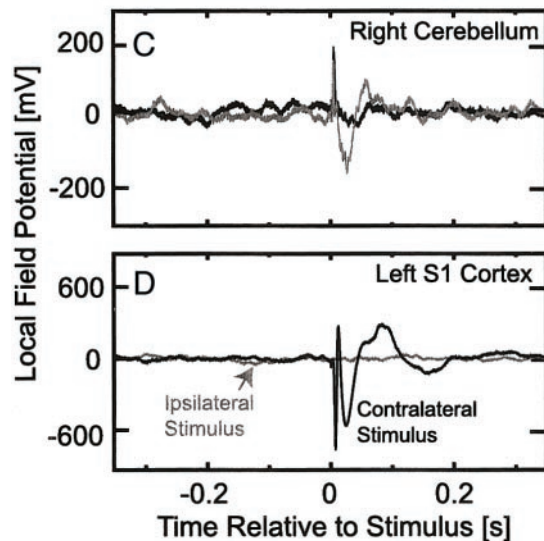
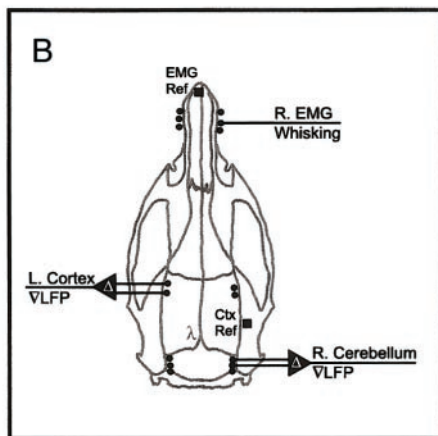
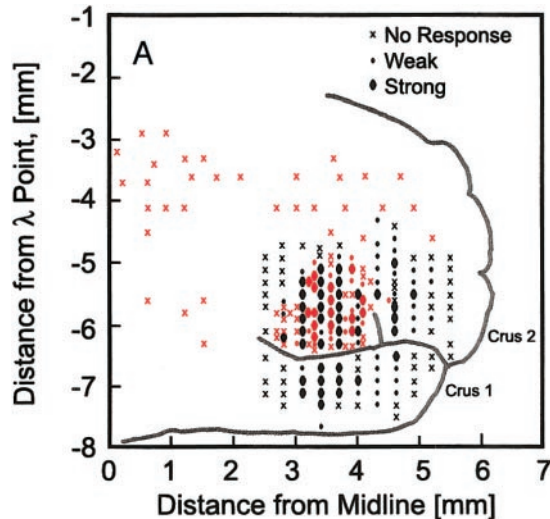
ipsilateral and contralateral aspects of each area, placed through 0.5-mm holes that were drilled through the skull at a nominal spacing of 1 mm. The final depth of each electrode was guided by the electrical signal measured in response to manual vibrissa deflection. Last, single microwires were implanted above occipital cortex and in temporal cortex; the latter served as a cortical reference site.

Vibrissa motion was inferred from the rectified EMG. Teflon-

insulated tungsten wire (0.002-in diam), with 1 mm of insulation stripped from the end, was threaded into the mystatial pad and set to lie about halfway through the whisker field. The same type of wire, with 5 mm of insulation stripped from the end, was implanted along the top surface of the nose to serve as an EMG reference site.

After a 10-day recovery from surgery, rats were trained to wait and then perch on the edge of a platform, while blindfolded, as a means to gain access to a food tube through which they received liquid food (0.5 ml/trial; LD-100; PMI Feeds) (Fee et al. 1997). Each trial was initiated when the rat approached the edge of the platform; after ~5 s, the tube was placed within reach of the rat. The behavioral state of the animal, e.g., whisking in air versus grooming the vibrissae, was inferred from concurrent video recordings in which the vibrissae were highlighted by darkfield illumination. Motion of the vibrissae was measured via the mystatial EMG (Carvell et al. 1991), the local field potential was measured at multiple neighboring locations (see following text) within the vibrissa areas of the cerebellum and S1 cortex. Upward of 50 trials were run per day.

The data for each animal were recorded over an ~2-mo period after surgery. At the end of this period, we verified the electrode placement by measuring the response at each electrode to deflection of vibrissae. The rats were placed under halothane anesthesia, as in the preceding text, and a clump of vibrissae were trapped in the openings of a fine mesh screen and deflected by a piezoelectric driver (Simons 1983) that delivered taps at 5-s intervals. The neuronal response was recorded and displayed as a trial average.



Recording and analysis

All electrical signals were buffered near the head of the animal with field effect transistors (NB Labs, Denville, TX). The signals from the cerebellum and parietal cortex were differentially amplified ($\times 12,800$) relative to the cortical reference, band-pass filtered between 0.1 Hz (RC high-pass filter) and 10 kHz (8-pole constant-phase low-pass filter; Frequency Devices), and digitized at 25 kHz with a 12-bit D/A converter (No. AT-MIO-16E-1, National Instruments). The difference between any two brain signals, low-pass filtering of the difference, and subsampling of the difference were performed numerically (Interactive Display Language; Research Systems). The EMG signals were differentially amplified relative to the nose reference, band-pass filtered between 200 Hz (4-pole Bessel high-pass filter) and 10 kHz (8-pole constant-phase low-pass filter; Frequency Devices), and digitized as in the preceding text. Rectification, low-pass filtering, and subsampling of the EMG data were performed numerically.

Differential local field potentials, denoted ∇ LFP, were calculated as the difference between pairs of LFPs that were measured from neighboring electrodes in the same area of the brain. The separation of the electrodes was $\sim 500 \mu\text{m}$ in the tangential plane. These measurements report the spatially averaged electrical activity in a volume of order

FIG. 2. Mapping and control experiments that relate to the proper placement of recording electrodes. *A*: maps of the electrical response in different areas of crus 1 and crus 2 to stimulation of 1 or multiple vibrissae. The recording electrode was lowered by ≤ 2 mm or until a response was apparent. Note the ~ 2 mm (A-P) \times 1.5 mm (M-L) region over which a strong response was obtained; this region was probed in the chronic measurements. *B*: schematic of the placement of extracellular electrodes. Two to three wires were placed in each mystatial pad to record the electromyogram (EMG); the reference was in the nose. Similarly, 2–3 microwires were placed in the vibrissa area of parietal cortex and in the vibrissa area of cerebellum; a low-impedance electrode in temporal cortex acted as the reference. All brain signals, ∇ LFP, refer to the numerical difference of the signals measured across 2 wires in the same brain area. *C*: stimulus-triggered average ($n = 500$) of the response of 1 cerebellar wire to a tap stimulus delivered either to contralateral vs. ipsilateral vibrissae (METHODS). Note the dominant ipsilateral response. *D*: stimulus-triggered average ($n = 500$) of the response of one neocortical wire to a tap stimulus delivered either to contralateral versus ipsilateral vibrissae (METHODS). Note the dominant contralateral response.

0.1 mm³, similar to that of a cortical column and estimated to contain on the order of 10⁴ neurons (Braitenberg and Schuz 1991).

Spectra power densities of individual time series, denoted $S_{xx}(f)$ in the following text, spectral coherence between different signals, denoted $C_{xy}(f)$ in the following text, and the SD of these measures, were calculated with the direct multi-taper spectral estimation techniques of Thomson (1982); see Cacciatore et al. (1999) for implementation. In brief, the spectral measures are defined by

$$S_{xx}(f) = \langle |\tilde{\mathbf{V}}_x|^2 \rangle$$

and

$$C_{xy}(f) = \frac{\langle \tilde{\mathbf{V}}_x \tilde{\mathbf{V}}_y^* \rangle}{\sqrt{\langle |\tilde{\mathbf{V}}_x|^2 \rangle \langle |\tilde{\mathbf{V}}_y|^2 \rangle}}$$

where $\langle \dots \rangle$ denotes an average over all instances and tapers, i.e.

$$\langle \tilde{\mathbf{V}} \tilde{\mathbf{U}} \rangle = \frac{1}{N} \frac{1}{K} \sum_{n=1}^N \sum_{k=1}^K \tilde{\mathbf{V}}^{(n,k)} \tilde{\mathbf{U}}^{(n,k)}$$

and

$$\tilde{\mathbf{V}}^{(n,k)} = \{\tilde{\mathbf{V}}^{(n,k)}(f)\}_{f=0}^{f_N} = \sum_{t=0}^T e^{j2\pi f t} \mathbf{w}^{(k)}(t) \mathbf{V}^{(n)}(t)$$

is the discrete Fourier transform of the time series, $\mathbf{V}^{(n)} \equiv \{\tilde{\mathbf{V}}^{(n)}(t)\}_{t=0}^T$, multiplied by the k th taper, $\mathbf{w}^{(k)} \equiv \{\mathbf{w}^{(k)}(t)\}_{t=0}^T$. The parameter N is the number of instances of the waveform ($\sim 10^2$ in the present work), K is the number of tapers or degrees of freedom in the spectral estimate (typically 5 in the present work), T is duration of the data trace (2 s in the present case), and $f_N = (2t_S)^{-1}$ is the Nyquist frequency where t_S is the time per point of the subsampled data (5 ms in the present work). In this procedure, the spectrum is averaged over a half-bandwidth Δf , which satisfies

$$\Delta f = \left(\frac{K+1}{2} \right) \frac{1}{T}$$

A special aspect of this spectral estimation techniques is that it minimizes the leakage between neighboring frequency bands. Additional smoothing, but no change in bandwidth, is obtained by averaging the spectra from multiple instances.

Standard deviations of the power spectra and the coherence are reported as jackknife estimates across trials (Thomson and Chave 1991). The confidence intervals for coherence were further computed for the multitaper estimates, as described (Jarvis and Mitra 2001), where the magnitude of the coherence will exceed $|C| > \sqrt{1 - P^{1/(NK-1)}}$ in $P \times 100\%$ of measurements, where NK is the total number of degrees of freedom. For a 95% confidence interval, which nominally corresponds to 2 SDs above chance in the limit of large numbers of independent samples, $P = 0.05$.

RESULTS

Maps and recording sites

The spatial localization of the stimulus-induced response in vibrissa S1 cortex is well described and, as a consequence of the lissencephalic structure of neocortex, is easily localized (Welker 1971; Woolsey et al. 1974). In contrast, the response in the cerebellum is more difficult to localize due to the convoluted nature of this cortex. As a means to verify the position of the sensory vibrissa representation, we measured the multi-unit response with Tungsten microelectrodes (METHODS) at a spatial resolution of $\leq 300 \mu\text{m}$ ($n = 4$ animals). We present the data for the two most extensive maps (Fig. 2A).

These show a strong response that is spread over many square millimeters of crus 1 and crus 2, similar in size and location to previous reports (Bower et al. 1981; Shambes et al. 1978).

Fidelity of the sensory signal in the LFPs

Chronic electrodes were placed in the center of the vibrissa area of crus 2 in cerebellum and in the vibrissa area in S1 cortex (Fig. 2B). We verified the position of the electrodes at the time of placement, as well as at the end of the data trials by recording the stimulus-induced response in the halothane-anesthetized animal. The result for a single cerebellar LFP electrode shows a trial-averaged response that is significantly greater for ipsilateral versus contralateral stimulation (Fig. 2C). Contrarywise, the cortical response is strong for contralateral stimulation but essentially unobservable for ipsilateral stimulation, consistent with previous reports for anesthetized animals (Armstrong-James and George 1988a,b).

Organization of behavioral states

Data were obtained from three animals. They performed their task with peak-to-peak whisking amplitudes typically $< 20^\circ$. The electrophysiological data were sorted based on two stereotypical behavioral states that were associated with exploration. These were "paused," a state of apparent transient immobility of the vibrissae as the animals maintained position on the perch, and "whisking." The whisking state was further divided into a state with relatively small-amplitude whisking ($< 10^\circ$) and head movements, denoted small whisking, and a state usually associated with searching for the food tube with whisking amplitudes of 10 to $\sim 20^\circ$, denoted medium whisking. The angle of 10° corresponds to the mode observed in an unconditioned whisking task using the head-fixed preparation of Zeigler (Sachdev et al. 2000). It is important not to confuse our definition of small whisking with twitching, in which the animal remains immobile and the thalamocortical electrical activity is highly synchronized (Nicoletis et al. 1995; Semba and Komisaruk 1984).

In addition to behavioral states during exploration, we identified a state that did not involve exploration, i.e., chewing, in which the animals made rhythmic jaw movements in association with eating. Chewing and other nonexploratory states were excluded from further analysis except for purposes of control measurements.

Cerebellar and neocortical responses

We consider the simultaneous electrical activity in the vibrissa sensory areas of cerebellum and S1 cortex with the motion of the vibrissae. We focus on the results from the animal with the correspondingly largest data set. The spectral coherence between the EMG and each brain response, as well as between the two brain areas, varied considerably between trials. Two examples, with spectral estimators computed in a sliding 2-s window, serve to illustrate the typical responses seen across all data sets. The first example contains two successive bouts of whisking (medium whisking, Fig. 3, A and B). The cerebellar ∇ LFP showed no remarkable change in amplitude during whisking (Fig. 3C), yet is clearly coherent with the first bout of whisking but only weakly coherent with the second bout (Fig. 3E). The neocortical ∇ LFP also appeared unremark-

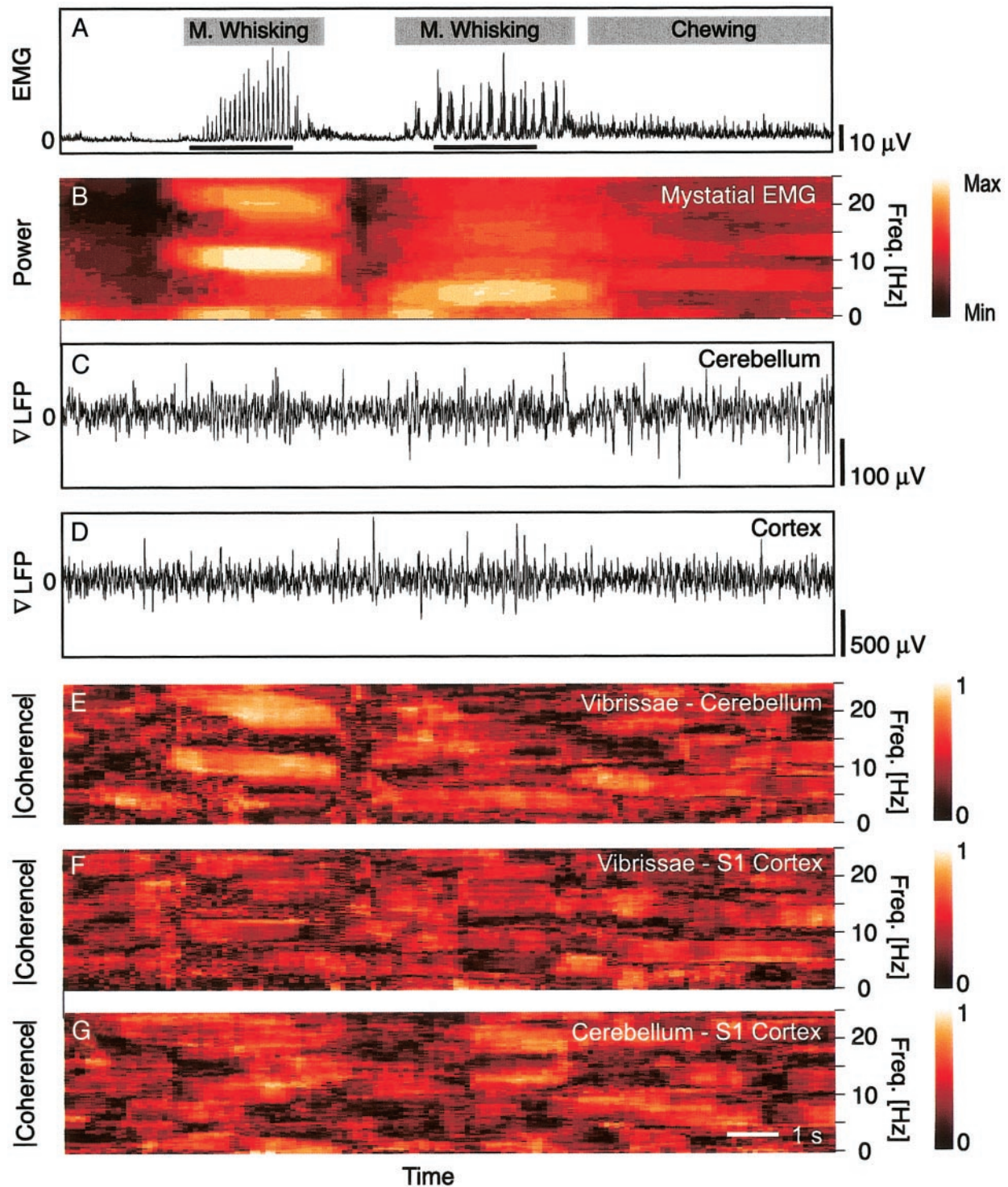


FIG. 3. Example of a single trial response of the relation between the mystatinal EMG and the cerebellar and cortical responses during epochs of sustained whisking. *A*: the rectified and filtered EMG, which reports vibrissa movement. The behavioral state of the animal, determined from video clips of the animal in the vicinity of the perch, is indicated by the gray bars. Note the change in frequency of whisking between successive bouts of medium whisking. *B*: the spectral power in the EMG as a function of time. A 2-s sliding window and a bandwidth of 2 Hz were used. The color white codes the highest magnitude and deep red the lowest. *C*: the spatially localized cerebellar response. *D*: the spatially localized cortical response. *E*: the magnitude of the coherence between the rectified EMG and the cerebellar response. Note that the coherence during the 1st whisking bout is stronger than that during the 2nd bout. A 2-s sliding window and a bandwidth of 2 Hz were used. White corresponds to 1 and deep red to 0. *F*: the magnitude of the coherence between the rectified EMG and the neocortical response. *G*: the magnitude of the coherence between the cerebellar and the neocortical responses.

able (Fig. 3D) and is less obviously modulated by whisking (Fig. 3F). Interestingly, the cerebellar and neocortical responses are partially coherent during both whisking bouts. For the first bout, there was weak but significant coherence at the ~10-Hz fundamental frequency of the whisking (Fig. 3G), while for the second bout, with an ~5-Hz fundamental frequency, the coherence lies at higher frequencies (Fig. 3G).

In the second example, we consider an epoch that contained strong bursts of ~7 Hz oscillatory activity in the S1 cortical and, over a more limited period, in the cerebellar recordings (Fig. 4, C and D). The latter burst overlaps with a bout of whisking (small whisking, Fig. 4, A and B). In this and related examples, the spectral coherence between the EMG and either the cerebellar or neocortical ∇ LFP was relatively high during

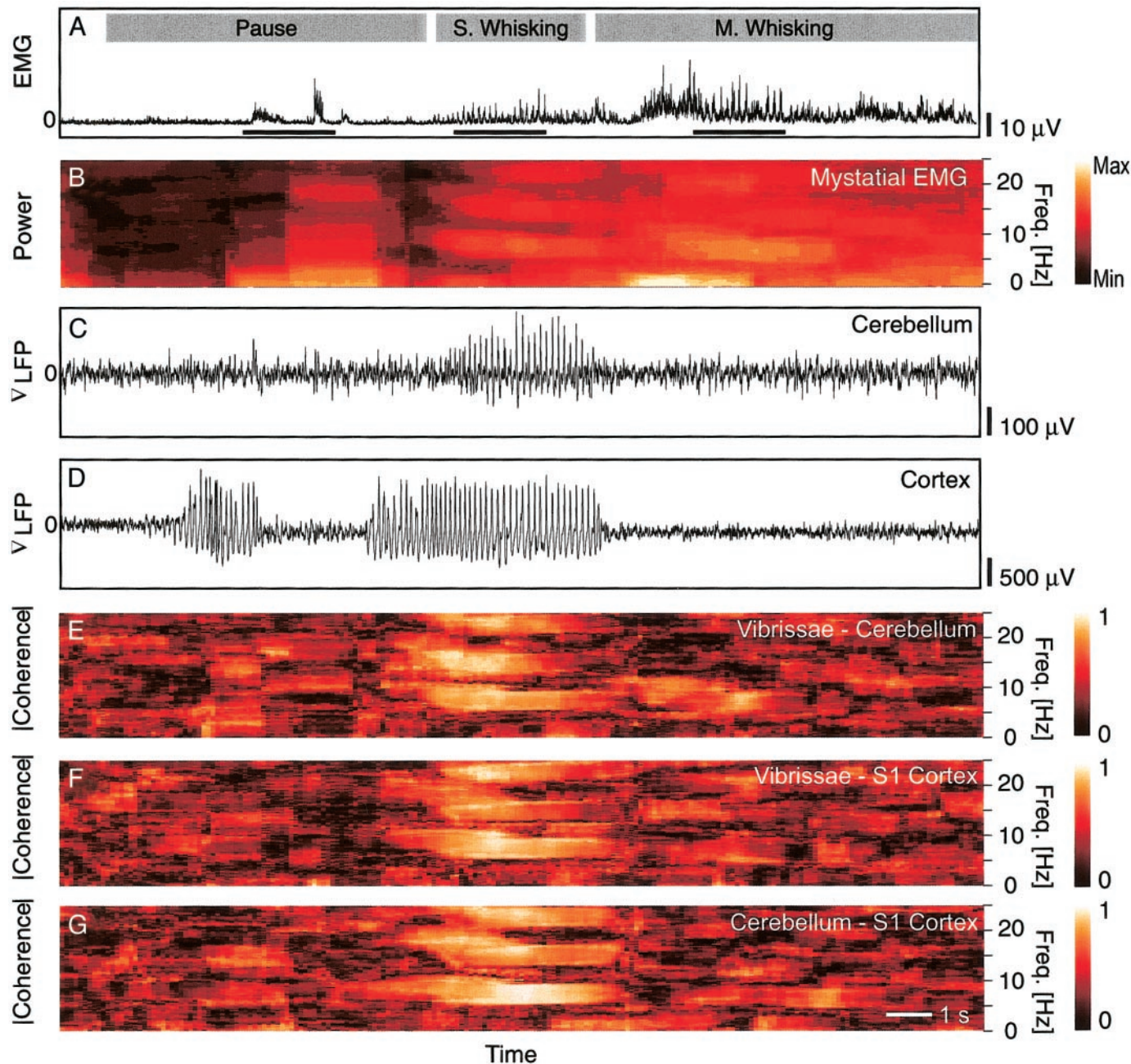


FIG. 4. Example of a single trial response of whisking and associated brain rhythms during an epoch of strong rhythmic activity internal to the brain. All spectral measures are as in Fig. 3. A: the rectified and filtered EMG. The behavioral state of the animal changes from pause to small whisking to medium whisking. Note that none of the whisking epochs contains a whisking “bout” by our definitions. B: the spectral power in the EMG as a function of time. Note the 2 strong peaks during the pause behavioral epoch. C: the spatially localized cerebellar response. Note the burst of oscillatory that occurs during small whisking. D: the spatially localized cortical response. Note the 2 bursts of oscillatory that occurs during small whisking. E: the magnitude of the coherence between the rectified EMG and the cerebellar response. Note the epoch of near unity coherence. F: the magnitude of the coherence between the rectified EMG and the neocortical response. Note the epoch of near unity coherence. G: the magnitude of the coherence between the cerebellar and the neocortical responses. Note the epoch of near unity coherence; the phase of the coherence during this epoch was nearly 0.

the burst (Fig. 4, *E* and *F*). Further, in this example there was significant coherence between the two vibrissa brain areas during both the pause and small whisking states (Fig. 4*G*), with a particularly large value during whisking. Collectively, the data of Figs. 3 and 4 illustrate the variability of the cerebellar and neocortical ∇ LFP responses between different whisking bouts.

In light of the substantial variability of the brain responses between whisking bouts (Figs. 3 and 4), we formed the composite response as a means to gain insight into the typical electrical behavior. We averaged the spectral power and the coherence across all trials of a given behavior (Fig. 5; $n = 120$ for pause; $n = 250$ for small whisking; and $n = 240$ for medium whisking). The change from pause to either whisking state was accompanied by the onset of a broad peak in the EMG that was centered near 7–8 Hz (Fig. 3*A*). There was a broad peak in the power spectrum of the cerebellar ∇ LFP during the pause state that was centered near 8–9 Hz. The amplitude of this peak was diminished by nearly two orders of magnitude in the whisking states; this corresponded to an order of magnitude drop in the amplitude of the ∇ LFP itself. In contrast to the severe drop in cerebellar oscillatory power on the onset of whisking, there was a strong increase in the amplitude of the spectral power in vibrissa S1 cortex with a broad peak centered near 8 Hz and a second peak centered near 16 Hz. Thus, on average, rhythmic whisking was accompanied by a decrease in cerebellar broadband oscillations but an increase in neocortical broadband oscillations at frequencies that overlapped with those involved with whisking.

Although cerebellar oscillations are observed during whisking (Fig. 5, *H* and *N*), the spectral coherence among the cerebellar ∇ LFP and the EMG was small, with $|C(f)| < 0.2$, where $|C|$ is the magnitude of the coherence with $0 < |C| < 1$ (Fig. 5, *J* and *P*). A similar situation occurred with the neocortical ∇ LFP and the EMG (Fig. 5, *I* and *O*), for which $|C(f)| < 0.15$ (Fig. 5, *K* and *Q*). In both cases, the magnitude of the coherence was significant ($P < 0.05$) at the peak frequencies of the EMG. Thus for example, only 0.1 of the local electrical activity in the vibrissa areas of the cerebellum or S1 cortex, as reported by the differential LFP, is phase-locked to rhythmic motion of the vibrissa when the animal whisks with a frequency of 8 Hz.

In contrast to the relatively low coherence between whisking and rhythmic electrical activation of cerebellum or neocortex, the coherence between the cerebellar ∇ LFP and the neocortical ∇ LFP was relatively high during epochs of whisking. When the animal was in the pause state, there was significant ($P < 0.01$) but small coherence between the cerebellum and S1 cortex, with $|C(f \cong 8 \text{ Hz})| \sim 0.1$ (Fig. 5*F*). This coherence increased for either small or medium whisking to $|C(f \cong 8 \text{ Hz})| \sim 0.3$ (Fig. 5*L*) and $|C(f \cong 16 \text{ Hz})| \sim 0.4$ (Fig. 5*R*). These data show that there is a relatively high level of synchronous signaling between the cerebellar and neocortical brain loops. This synchrony appears to be at most only partially locked to the occurrence of whisking.

Our data show that whisking spans a broad range of frequencies, from ~ 5 to 15 Hz (Fig. 3, *G* and *M*), as animals whisk freely in air. We emphasize that the relatively low-frequency EMG signals, such as that in the medium whisking bout shown in Fig. 3*A*, are true whisker movements. In partic-

ular, these signals are not, per se, related to chewing, for which the EMG has a substantially reduced amplitude (Fig. 5*A*, *inset*).

Global coherence

The preceding results show that the coherence between the cerebellar and neocortical ∇ LFP was relatively high during epochs of whisking in both low- and high-frequency bands. The high-frequency (15–20 Hz) band is poorly represented in the EMG (Fig. 5, *G* and *M*). Thus one possibility is that the spectral power and internal coherence associated with this band is a general feature of arousal and is not specific to either whisking or vibrissa areas in the brain. To test this possibility, we calculated two measures of field potential, denoted the Δ LFP, that spanned the brain and encompassed multiple sensory modalities. The first measure of the Δ LFP spanned the parietal to the occipital areas of the neocortex (Fig. 6*A*). We found that the high-frequency component was essentially absent in the spectral power of the global Δ LFP signal for any of the exploratory states, i.e., paused (Fig. 6*B*), small whisking (Fig. 6*C*), or medium whisking (Fig. 6*C*). The second measure of the Δ LFP spanned parietal cortex to the cerebellum (Fig. 6*D*). We again found that the high-frequency component was essentially absent in the spectral power of the global Δ LFP signal for the exploratory states (Fig. 6, *E–G*). These data imply that the power in the local cerebellar and neocortical ∇ LFP signals at high frequencies, and, by inference, the coherence between these signals at high frequencies, is specifically related to whisking.

Dominant pattern of spectral coherence during whisking

Our analysis so far concerned the magnitude of the pair-wise coherence among the three recording sites (Fig. 1). We now consider the spatial distribution of the phase as well as the magnitude across all sites as a means to gain insight into the patterns of coherence that emerge when animals whisk freely in air. The set of coherences between all pair-wise combinations of recording sites at a particular frequency, f , can be expressed in the form of a 3×3 Hermitian matrix whose elements are the values of the coherence, $C_{xy}(f)$. We denote this complex matrix $\mathbf{C}(f)$, which can formally be expanded as $\mathbf{C}(f) = \mathbf{U}(f) \mathbf{\Lambda}(f) [\mathbf{U}(f)]^\dagger$, where the columns of $\mathbf{U}(f)$, denoted $\mathbf{U}_i(f)$, are the eigenmodes, the diagonal elements of $\mathbf{\Lambda}(f)$, denoted $\lambda_i(f)$, are the eigenvalues, and “ \dagger ” signifies Hermitian conjugation. The dominant mode at each frequency was found as the leading eigenvalue of the matrix of coherences.

For the spectral bands from 6 to 10 Hz and from 15 to 19 Hz, the leading eigenmode captured $\sim 75\%$ of the total variance. These frequency bands correspond to peaks in the two independent coherence spectra (Fig. 5, *L* and *R*). The leading component of the eigenmodes was averaged within a frequency band, and the average modes are shown in Fig. 7, *A* and *B*, respectively (the length of the arrow is proportional to the magnitude of the response and the direction of the arrow is proportional to the relative phase-angle). The essential result is that the phase of the vibrissa rhythm substantially lags that of the brain areas for the 6- to 10-Hz band, with a phase difference of 0.55π rad (Fig. 7*A*). The difference corresponds to a peak in the brain signals when the whiskers begin to protract

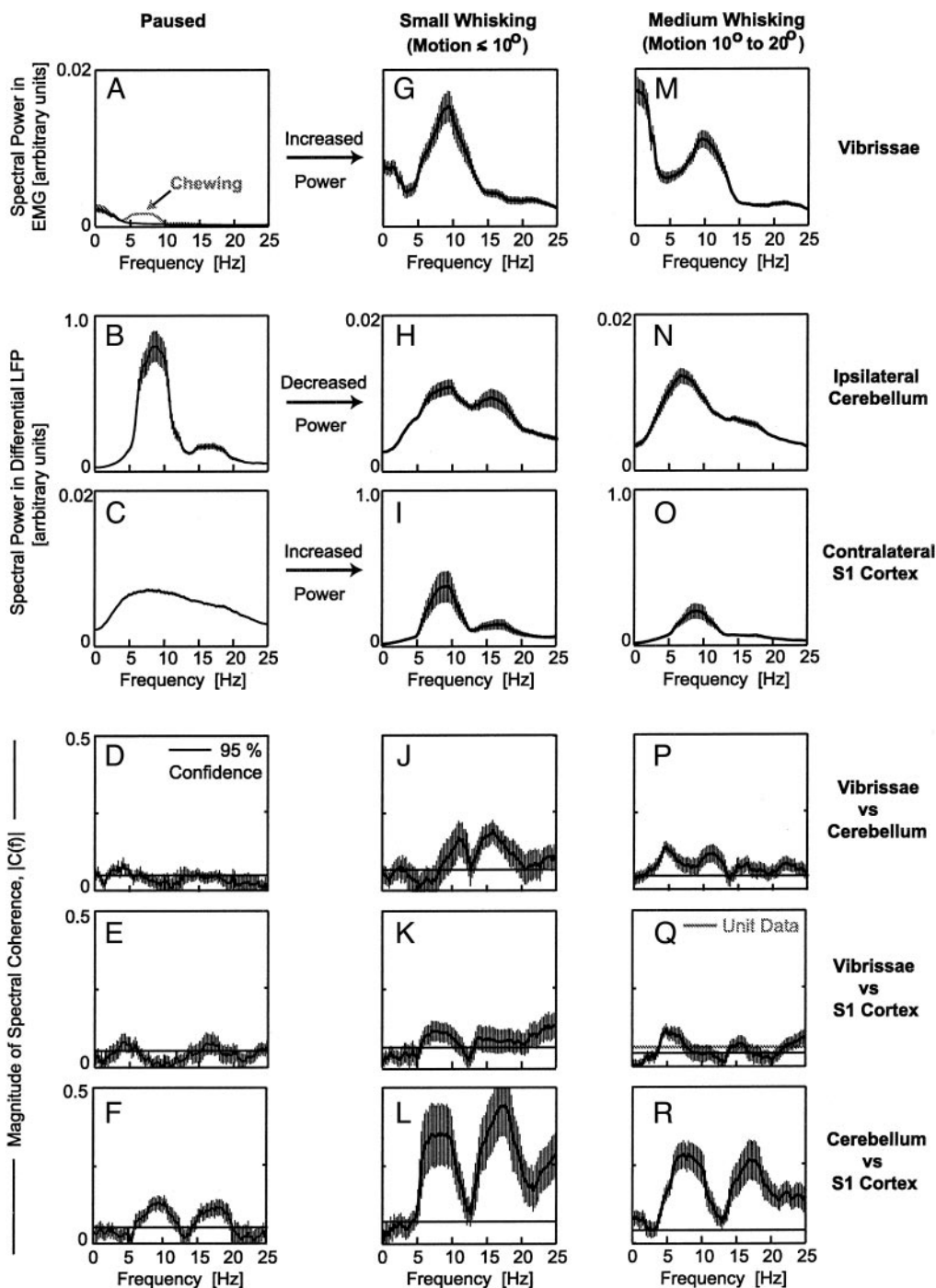


FIG. 5. The trial-averaged spectral power in vibrissa movement (rectified EMG) and in the cerebellar and neocortical responses, ∇ LFP, during different behaviors along with the magnitude of the spectral coherence among these measures. The error bars are ± 1 SD, computed as jackknife estimates over all trails. The 95% confidence intervals were computed under the assumption of independent events. Note the agreement among the 2 statistics, i.e., 95% confidence is approximately equal to 2σ . A–F: epochs during which the animal pauses, and stays essentially immobile, during exploration ($n = 259$). The essentially flat EMG confirms the absence of whisking. Note also the strong spectral peak in the cerebellar response. *Inset*: the EMG response during chewing as a control to show that it does not contribute to the vibrissa response. G–L: epochs associated with small whisking movements during exploration ($n = 134$). Note the severe drop in cerebellar spectral power and the increase in neocortical power between paused and small whisking. M–R: epochs associated with medium whisking movements during exploration ($n = 357$). The response is qualitatively similar to that during small whisking.

from the retracted position. In contrast, the phase of the vibrissae are nearly commensurate with that of the brain areas for the 15- to 19-Hz band, with a phase difference of $<0.03 \pi$ rad

(Fig. 7B). These phase relations, near synchronous electrical activity in vibrissa areas of cerebellum and neocortex in both frequency bands with a phase lag between brain activity and

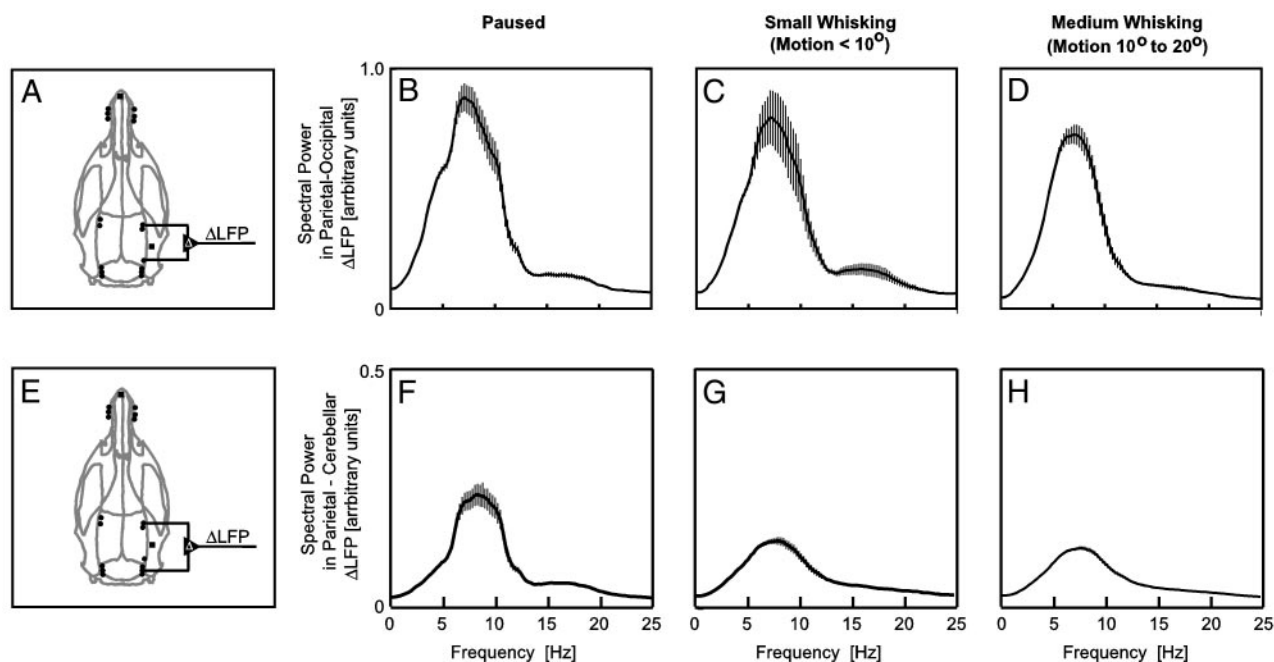


FIG. 6. The magnitude of the trial-averaged spectral power of the global LFP recorded across brain areas. This differential signal is denoted as the Δ LFP. *A*: schematic of the placement of extracellular electrodes for recording the Δ LFP between parietal and occipital cortex. The parietal signal was an average of 3 microwires that were placed in the vibrissa area of parietal cortex (Fig. 3*B*) and the occipital signal was from a single microwire. *B*: the spectral power for epochs during which the animal is paused ($n = 259$). *C*: the spectral power for epochs associated with small whisking during exploration ($n = 134$). *D*: the spectral power for epochs associated with medium whisking during exploration ($n = 357$). *E*: schematic of the placement of extracellular electrodes for recording the Δ LFP between parietal cortex and the cerebellum. The parietal signal was an average of 3 microwires, as in *A*, and the cerebellar signal was an average of 3 microwires in the vibrissa area of the cerebellum (Fig. 3*B*). *F*: the spectral power for epochs during which the animal is paused. *G*: the spectral power for epochs associated with small whisking. *H*: the spectral power for epochs associated with medium whisking.

vibrissa motion only for the low frequency band, were observed in all three animals.

DISCUSSION

We observed that the internal coherence among the field potential activity of vibrissa sensory areas in the brain is relatively high as the animals whisk in search of a target. Thirty to 40% of the activity between vibrissa cerebellum and neocortex is correlated during such whisking (Fig. 4, *L* and *R*). In contrast to the high internal coherence, there was significant yet small coherence between the rhythmic activity in either vibrissa cerebellum or vibrissa S1 cortex and rhythmic whisking (Fig. 5, *J* and *P*, and *K* and *Q*, respectively). These data imply that the major fraction of coherent signaling between vibrissa cerebellum and vibrissa S1 cortex is incoherent with whisking, even though signaling among the brain regions and whisking share common frequency bands (Fig. 7, *A* and *B*).

Relation to previous cerebellar studies

The participation of the cerebellum in vibrissa somatosensation was highlighted by Welker and colleagues (Shambes et al. 1978; see also Bower et al. 1981; Kennedy et al. 1966; Morissette and Bower 1996), and the role of signaling within the vibrissa sensory area of the cerebellum was addressed in the awake animal studies of Hartmann and Bower (1998).

Here, we find that the vibrissa areas of cerebellum exhibited broadband oscillations, i.e., in the 5- to 10-Hz and 15- to 20-Hz ranges, in both the pause state, during which the rat is immobile for a period of ≥ 1 s during exploration, as well as in the two whisking states (Fig. 5, *B*, *H*, and *N*). Critically, the cerebellar oscillation in the whisking states is significantly modulated in phase with both rhythmic whisking and electrical oscillations in vibrissa neocortex (Fig. 5, *L* and *R*).

Our observation of spectral power in the ~ 6 - to 10-Hz frequency range (Fig. 5, *B*, *H*, and *N*) is consistent with that found in recordings from semi-intact or anesthetized preparations from a variety of species (Bell and Kawasaki 1972; Bloedel and Ebner 1984; Llinas and Sasaki 1989; Llinas and Yarom 1986) as well as the awake behaving rat (Hartmann and Bower 1998; Lang et al. 1999; Welsh et al. 1995). In agreement with the conclusions from the studies of Hartmann and Bower (1998), we found that oscillatory activity in the pause state was particularly strong (Fig. 5*B*). However, in contrast to the claims by these authors, we found that such activity persists when the animals are mobile and whisking, albeit at an amplitude that is reduced by a factor of 7–8 from that in the pause state (cf. Fig. 5, *B* with *H* and *N*). This difference in conclusions appears to result from the increased instrumental sensitivity in the present study.

Strong rhythmic cerebellar activity is present in the pause state, while cortical activity is both weak and spectrally flat (Fig. 5). This result supports the conclusion of Llinas and Welsh (Lang et al. 1999; Welsh et al. 1995) that was derived

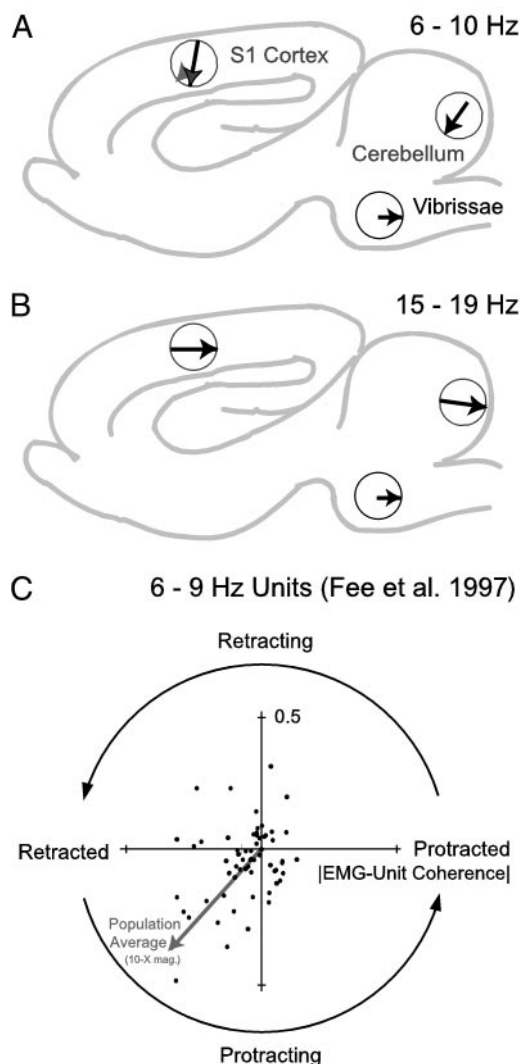


FIG. 7. Summary of strength and relative phase between the vibrissae, the vibrissa area of cerebellum, and the vibrissa area of S1 cortex. *A*: the magnitudes and phases of the dominant mode of the coherence between 6 and 10 Hz. The 3 elements of $U_1(f)$ are plotted as phasors as a function of frequency; the length of each arrow is the magnitude of the coherence and the direction refers to the relative phase. Note that different brain areas are synchronized among each other but out of phase with whisking. The light gray arrow for the vibrissa area of S1 cortex represents the phase derived from the spike data in *C*. *B*: the magnitudes and phases of the dominant mode between 15 and 19 Hz. Note that different brain areas are essentially synchronized among each other. *C*: reevaluation of the single unit data of Fee et al. (1997), obtained during a whisking task similar to that in the present study. The magnitude and phase of the coherence between the spike signal and the peak of the EMG is plotted on polar coordinates. There are 107 units in this average, of which 61 had values of coherence that were significantly larger than 0. The average coherence had a magnitude of 0.049 with a phase of $\Delta\psi = -0.74$ rad.

from studies on cerebellar activity in animals trained in a tongue licking task. In particular, we echo their conclusion that “the olivocerebellar system is capable of generating periodic patterns of synchronous activity in the awake animal.” We cannot, however, rule out the possibility that the rhythmic drive to the cerebellum lies outside this hindbrain system, although a more likely scenario is that a olivocerebellar oscillator simply locks with other oscillators in the vibrissa sensorimotor system.

Relation to past work on unit recording from vibrissa S1 cortex

The relationship between the EMG and the spike output from units in vibrissa S1 cortex for rats trained to perform the same task as used in the present work has been reported (Fee et al. 1997). In that study, the electrodes were lowered and signals were collected and stored without bias as to the response properties of the units. The final single-unit responses exhibited a wide distribution of responses to changes in vibrissa position. A significant correlation between the spike arrival times and the peaks of the EMG was observed for 57% of the single units ($n = 107$). The magnitude of the coherence at the whisking frequency varied between units and ranged from undetectable, $|C| < 0.02$, to a value of $|C| = 0.65$. The phase of the coherence was distributed among all angles but biased between $-\pi/2$ and π rad (Fig. 7C). For some units, the combination of spike rate and correlation were high enough so that the output of a single unit could reliably predict the position of the vibrissae.

The mean phase between the vibrissa position and the cortical single-unit response was determined from the published data (Fee et al. 1997) to compute the vector average of the coherence between the EMG and unit response. We found that the magnitude of the average coherence was 0.05 at the ~ 8 -Hz whisking frequency in that experiment (Fig. 7C), equal to the same value for the ∇ LFP data at 8 Hz (Fig. 5Q). We further found that the phase-angle between the EMG and the spike data were 0.72π rad, close to the value 0.55π rad that found for the LFP data (cf. Fig. 7A). We conclude that the ∇ LFP data faithfully reports a signal given by the average unit response and that the average modulation of the electrical activity in vibrissa S1 cortex by whisking is < 0.1 . It remains to be determined if the modulation in spike rate is increased on continual contact during whisking, as occurs, e.g., in a roughness discrimination task (Carvell and Simons 1990; Guic-Robles et al. 1989).

The relatively small coherence between whisking in air and the electrical response in vibrissa S1 cortex (Fig. 3Q) may appear paradoxical in light of the large, punctate response that is reported for stimulus-induced activity in S1 cortex with anesthetized animals (Armstrong-James and Fox 1987; Armstrong-James et al. 1992; Simons 1978, 1985; Welker et al. 1993), sessile animals (Nicolelis et al. 1995), and awake but immobilized animals (Kleinfeld et al. 2000; Sachdev et al. 1998). We note only that the cortical response during active movement of the vibrissae need not be the same as the response to direct stimulation.

Functional role of the intrinsic oscillations

Our results indicate that there is substantial internal signaling between the vibrissa areas of cerebellum and S1 cortex within the 5- to 10-Hz and 15- to 20-Hz frequency bands. The magnitude of this signaling is tied to the presence of whisking although it is not phase locked to the whisking motion. The coexistence of broadband signals that share the same frequency band is a common feature of modern communication systems (Viterbi 1995). However, we can only speculate about the nature of the signaling between these areas in the sensorimotor

loops. One possibility is that the internal signal may be a reference signal that is part of a phase-sensitive detection scheme to report vibrissa position (Ahissar and Kleinfeld 2002; Ahissar et al. 1997; Kleinfeld et al. 1999; Marr 1969). In this scheme, the internal signal is used to demodulate an incoming rhythmic input such that an error signal is generated when the vibrissa change their motion, as occurs on contact with an object.

We thank T. H. Bullock and F. F. Ebner for comments on early aspects of this work, E. Brown and M. R. Jarvis for introducing us to asymptotic estimates of confidence intervals, S. Hefler for assistance with the animal husbandry and histology, and B. Friedman for comments on the manuscript.

This work was supported by the Whitehall Foundation, the National Institute of Mental Health, and a National Institutes of Health predoctoral training grant to S. M. O'Connor.

Present address of S. M. O'Connor: Science Applications International Corp., San Diego, CA 92037.

REFERENCES

- AHISSAR E, HAIDARLIU S, AND ZACKENHOUSE M. Decoding temporally encoded sensory input by cortical oscillators and thalamic phase comparators. *Proc Natl Acad Sci USA* 94: 11633–11638, 1997.
- AHISSAR E AND KLEINFELD D. Closed loop neuronal computations: focus on vibrissa somatosensation in rat. *Cerebral Cortex*. In press.
- ARMSTRONG-JAMES M AND FOX K. Spatiotemporal convergence and divergence in the rat S1 "barrel" cortex. *J Comp Neurol* 263: 265–281, 1987.
- ARMSTRONG-JAMES M, FOX K, AND DAS-GUPTA A. Flow of excitability within barrel cortex on striking a single vibrissa. *J Neurophysiol* 68: 1345–1356, 1992.
- ARMSTRONG-JAMES M AND GEORGE MJ. Bilateral receptive fields in rat Sml cortex. *Exp Brain Res* 70: 155–165, 1988a.
- ARMSTRONG-JAMES M AND GEORGE MJ. Influence of anesthesia on spontaneous activity and receptive field size of single units in rat Sml neocortex. *Exp Neurol* 99: 369–387, 1988b.
- BELL CC AND KAWASAKI T. Relations among climbing fiber responses of nearby Purkinje cells. *J Neurophysiol* 35: 155–169, 1972.
- BLOEDEL JR AND EBNER TJ. Rhythmic discharge of climbing fiber afferents in response to natural peripheral stimuli in the cat. *J Physiol (Lond)* 352: 129–146, 1984.
- BOWER JM, BEERMAN DH, GIBSON JM, SHAMBES GM, AND WELKER W. Principles of organization of a cerebro-cerebellar circuit. Micromapping the projections from cerebral (SI) to cerebellar (granule cell layer) tactile areas of rats. *Brain Behav Evol* 18: 1–18, 1981.
- BRAITENBERG V AND SCHUZ A. *Anatomy of the Cortex: Statistics and Geometry*. Berlin: Springer-Verlag, 1991.
- CACCIATORE TW, BRODFUEHER PD, GONZALEZ JE, JIANG T, ADAMS SR, TSIEH RY, KRISTAN WB JR, AND KLEINFELD D. Identification of neural circuits by imaging coherent electrical activity with FRET-based dyes. *Neuron* 23: 449–459, 1999.
- CARVELL GE AND SIMONS DJ. Biometric analyses of vibrissal tactile discrimination in the rat. *J Neurosci* 10: 2638–2648, 1990.
- CARVELL GE, SIMONS DJ, LICHTENSTEIN SH, AND BRYANT P. Electromyographic activity of mystacial pad musculature during whisking behavior in the rat. *Somatosens Mot Res* 8: 159–164, 1991.
- CHAPIN JK AND LIN C-S. Mapping the body representation in the SI cortex of anesthetized and awake rats. *J Comp Neurol* 229: 199–213, 1984.
- DORFL J. The musculature of the mystacial vibrissae of the white mouse. *J Anat* 135: 147–154, 1982.
- DORFL J. The innervation of the mystacial region of the white mouse. A topographical study. *J Anat* 142: 173–184, 1985.
- ECKHORN R, BAUER R, JORDAN W, BRROSCH M, KRUSE W, MUNK M, AND REITBOECK HJ. Coherent oscillations: a mechanism of feature linking in the visual cortex? *Biol Cybern* 60: 121–130, 1988.
- FEE MS, MITRA PP, AND KLEINFELD D. Central versus peripheral determinates of patterned spike activity in rat vibrissa cortex during whisking. *J Neurophysiol* 78: 1144–1149, 1997.
- FRIEDMAN-HILL S, MALDONADO PE, AND GRAY CM. Dynamics of striate cortical activity in the alert macaque. I. Incidence and stimulus dependence of gamma-band neuronal oscillations. *Cereb Cortex* 10: 1105–1116, 2000.
- FRIES P, REYNOLDS JH, RORIE AE, AND DESIMONE R. Modulation of oscillatory neuronal synchronization by selective attention. *Science* 291: 1560–1563, 2001.
- GRAY CM, KONIG P, ENGEL AK, AND SINGER W. Oscillatory responses in cat visual cortex exhibit inter-columnar synchronization which reflects global stimulus properties. *Nature* 338: 334–337, 1989.
- GUIC-ROBLES E, VALDIVIESO C, AND GUAJARDO G. Rats can learn a roughness discrimination using only their vibrissal system. *Behav Brain Res* 31: 285–289, 1989.
- HARTMANN MJ AND BOWER JM. Oscillatory activity in the cerebellar hemispheres of unrestrained rats. *J Neurophysiol* 80: 1598–1604, 1998.
- HATTOX AM, PRIEST CA, AND KELLER A. Functional circuitry involved in the regulation of whisker movements. *J Comp Neurol* 442: 266–276, 2001.
- IZHIKEVICH EM. Weakly connected quasi-periodic oscillations, FM interactions, and multiplexing in the brain. *SIAM J App Math* 59: 2193–2223, 1999.
- JARVIS MR AND MITRA PP. Sampling properties of the spectrum and coherency of sequences of action potentials. *Neural Computat* 13: 717–749, 2001.
- KENNEDY TT, GRIMM RJ, AND TOWE AL. The role of cerebral cortex in evoked somatosensory activity in cat cerebellum. *Exp Neurol* 14: 13–32, 1966.
- KLEIN B AND RHOADES R. The representation of whisker follicle intrinsic musculature in the facial motor nucleus of the rat. *J Comp Neurol* 232: 55–69, 1985.
- KLEINFELD D, BERG RW, AND O'CONNOR SM. Anatomical loops and their relation to electrical dynamics in relation to whisking by rat. *Somatosens Mot Res* 16: 69–88, 1999.
- KLEINFELD D, SACHDEV RNS, AND EBNER FF. Rhythmic stimulation of the vibrissae modulates the spike rate of units in primary motor cortex of awake rat. In: *Society for Neuroscience Annual Meeting*, New Orleans, LA, 2000.
- KREITER AK AND SINGER W. Stimulus-dependent synchronization of neuronal responses in the visual cortex of the awake macaque monkey. *J Neurosci* 16: 2381–2396, 1996.
- LANG EJ, SUGIHARA I, WELSH JP, AND LLINAS R. Patterns of spontaneous Purkinje cell complex spike activity in the awake rat. *J Neurosci* 27: 2718–2739, 1999.
- LLINAS R AND SASAKI K. The functional organization of the olivo-cerebellar system as examined by multiple Purkinje cell recordings. *Eur J Neurosci* 1: 587–602, 1989.
- LLINAS R AND YAROM Y. Oscillatory properties of guinea pig inferior olivary neurons and their pharmacological modulation: an in vitro study. *J Physiol (Lond)* 376: 163–182, 1986.
- MARR D. A theory of cerebral cortex. *J Physiol (Lond)* 202: 437–470, 1969.
- MIYASHITA E, KELLER A, AND ASANUMA H. Input-output organization of the rat vibrissal motor cortex. *Exp Brain Res* 99: 223–232, 1994.
- MORISSETTE J AND BOWER JM. Contribution of somatosensory cortex to responses in the rat cerebellum granule cell layer following peripheral tactile stimulation. *Exp Brain Res* 109: 240–250, 1996.
- NATIONAL INSTITUTES OF HEALTH. *Guide for the Care and Use of Laboratory Animals*. Bethesda: National Institutes of Health, 1985, NIH Publication 85-23.
- NICOLELIS MAL, BACCALA LA, LIN RCS, AND CHAPIN JK. Sensorimotor encoding by synchronous neural ensemble activity at multiple levels of the somatosensory system. *Science* 268: 1353–1358, 1995.
- PRECHTL JC. Visual motion induces synchronous oscillations in turtle visual cortex. *Proc Natl Acad Sci USA* 91: 12467–12471, 1994.
- PRECHTL JC, COHEN LB, MITRA PP, PESARAN B, AND KLEINFELD D. Visual stimuli induce waves of electrical activity in turtle cortex. *Proc Natl Acad Sci USA* 94: 7621–7626, 1997.
- ROELFSEMA PR, ENGEL AK, KONIG P, AND SINGER W. Visuomotor integration is associated with zero time-lag synchronization among cortical areas. *Nature* 385: 157–161, 1997.
- SACHDEV RNS, JENKINSON EW, AND EBNER FF. Response properties of barrel field neurons in awake, behaving rat. In: *Society for Neuroscience Annual Meeting*, Los Angeles, CA, 1998.
- SACHDEV RNS, JENKINSON E, ZEIGLER HP, AND EBNER FF. Sensorimotor plasticity in the rodent vibrissa system. In: *The Mutable Brain*, edited by Kass J. San Diego: Academic, 2000, p. 123–164.
- SEMBA K AND KOMISARUK BR. Neural substrates of two different rhythmical vibrissal movements in the rat. *Neuroscience* 12: 761–774, 1984.
- SHAMBES GM, GIBSON JM, AND WELKER W. Fractured somatotopy in granule cell tactile areas of rat cerebellar hemispheres revealed by micromapping. *Brain Behav Evol* 15: 94–140, 1978.
- SIMONS DJ. Response properties of vibrissal units in rat S1 somatosensory neocortex. *J Neurophysiol* 41: 798–820, 1978.

- SIMONS DJ. Multi-whisker stimulation and its effects on vibrissa units in rat SmI barrel cortex. *Brain Res* 276: 178–182, 1983.
- SIMONS DJ. Temporal and spatial integration in the rat SI vibrissa cortex. *J Neurophysiol* 54: 615–635, 1985.
- THOMSON DJ. Spectral estimation and harmonic analysis. *Proc IEEE* 70: 1055–1096, 1982.
- THOMSON DJ AND CHAVE AD. Jackknifed error estimates for spectra, coherences, and transfer functions. In: *Advances in Spectrum Analysis and Array Processing*, edited by Shykin S. Englewood Cliffs, NJ: Prentice Hall, 1991, p. 58–113.
- VITERBI AJ. *CDMA: Principles of Spread Spectrum Communication*. New York: Addison Wesley Longman, 1995.
- WELKER C. Microelectrode delineation of fine grain somatotopic neocortex of the rat. *Brain Res* 26: 259–275, 1971.
- WELKER E, ARMSTRONG-JAMES M, VAN DER LOOS H, AND KRAFTSIK R. The mode of activation of a barrel column: response properties of single units in the somatosensory cortex of the mouse upon whisker deflection. *Eur J Neurosci* 5: 691–712, 1993.
- WELSH JP, LANG EJ, SUGIHARA I, AND LLINAS R. Dynamic organization of motor control within the olivocerebellar system. *Nature* 374: 453–457, 1995.
- WOOLSEY TA, WELKER C, AND SCHWARTZ RH. Comparative anatomical studies of the SmI face cortex with special reference to the occurrence of “barrels” in layer IV. *J Comp Neurol* 164: 79–94, 1974.